Journal of Integrative Agriculture 2026, 25(3): 1137–1149

KeAi
CHINESE ROOTS
GLOBAL IMPACT

Available online at ScienceDirect

Journal of Integrative Agriculture



RESEARCH ARTICLE

ACSL4 is a target for β-hydroxybutyrate-induced increase in fatty acid content and lipid droplet accumulation in bovine mammary epithelial cells

Ming Li[1], Jingjing Wang[2], Jia'nan Wen[2], Juan J. Loor[3], Qianming Jiang[3], Jingyi Wang[1], Huijing Zhang[1], Yue Yang[1], Wei Yang[4], Bingbing Zhang[2], Chuang Xu[1#]

[1] *College of Veterinary Medicine, China Agricultural University, Beijing 100193, China*
[2] *College of Life Science and Technology, Heilongjiang Bayi Agricultural University, Daqing 163319, China*
[3] *Mammalian NutriPhysio Genomics, Department of Animal Sciences and Division of Nutritional Sciences, University of Illinois, Urbana 61801, USA*
[4] *College of Animal Science and Veterinary Medicine, Heilongjiang Bayi Agricultural University, Daqing 163319, China*

Highlights

- ACSL4 regulates fatty acid synthesis and accumulation in BMECs during ketosis.
- BHB leads to an increase in ACSL4 expression, which in turn increases fatty acid content and lipid droplet accumulation, and inhibiting ACSL4 would reduce the effects of BHB.
- ACSL4 suppression decreases ROS, improves mitochondrial function, and increases fatty acid oxidation.

Abstract

Ketosis, a common metabolic disease during early lactation, is associated with high circulating levels of β-hydroxybutyrate (BHB). A portion of BHB that reaches the mammary gland is utilized as precursor for synthesis of fatty acids. Recent findings from nonruminant studies revealed that long chain fatty acyl-CoA ligase 4 (ACSL4) could play a role in the regulation of cellular fatty acid metabolism, but the mechanisms by which ACSL4 mediates cellular lipid metabolism in response to BHB remains unclear. To achieve the aims, we conducted *in vivo* or *in vitro* analyses using bovine mammary gland biopsies and the immortalized mammary epithelial cell line (MAC-T). The *in vivo* study (n=6 cows per group) involved healthy cows (plasma BHB<0.60 mmol L^{-1}) or ketotic cows (plasma BHB>2.0 mmol L^{-1}) from which mammary gland tissue was biopsied. *In vitro*, MAC-T cells were challenged with 0, 0.3, 0.6, 1.2, or 2.4 mmol L^{-1} BHB for 24 h to determine an optimal dose. Subsequently, MAC-T were incubated with 1.2 mmol L^{-1} BHB for 0, 3, 6, 12, 24, or 48 h. Furthermore, MAC-T cells were treated with small interfering ACSL4 (siACSL4) for 24 h or ACSL4 overexpression plasmid (pcACSL4) for 36 h followed by a challenge with 1.2 mmol L^{-1} BHB for 24 h. Results showed that increased mRNA and protein abundance of lipogenic genes were linked to both mammary gland and *in vitro* challenge with BHB. BHB increased fatty acid content by activating ACSL4 expression, whereas inhibition of ACSL4 reduced BHB-induced reactive oxygen species (ROS) overproduction, enhancement of mitochondrial membrane potential, increase in fatty acid content, and lipid droplet accumulation. Furthermore, we also elevated ACSL4 expression with an overexpression plasmid to clarify its molecular role in response to BHB challenge. ACSL4 overexpression enhances BHB-induced lipid droplet accumulation by increased fatty acid content. Overall, the information showed that ACSL4 is crucial for the process of producing fatty acids from exogenous BHB. Reduced ACSL4 decreased fatty acid content and lipid droplet accumulation, improved mitochondrial function, directed more fatty acids towards oxidation. Thus, ACSL4 plays an important role in determining the fate of intracellular fatty acids and BHB in BMECs.

Keywords: bovine mammary epithelial cells, fatty acid content, ketosis, BHB, ACSL4

Received 10 September 2023; Received in revised form 7 April 2024; Accepted 26 September 2024; Available online 5 December 2024
Ming Li, E-mail: liming5697@163.com; [#]Correspondence Chuang Xu, E-mail: xuchuang7175@163.com

© 2026 CAAS. Publishing services by Elsevier B.V. on behalf of KeAi Communications Co. Ltd. This is an open access article under the CC BY-NC-ND license (http://creativecommons.org/licenses/by-nc-nd/4.0/). Peer review under responsibility of Editorial Board of *Journal of Integrative Agriculture*.
doi: 10.1016/j.jia.2024.12.004

1. Introduction

Ketosis is one of the most prevalent metabolic diseases of dairy cows during early lactation (Littledike *et al.* 1981). In this period, a combination of an abrupt increase in milk production and insufficient energy intake results in negative energy balance (NEB) causing body fat reserve mobilization that raises concentrations of non-esterified fatty acids (NEFA) (Baird 1982). Incomplete oxidation of NEFA are metabolized to ketone bodies (primarily β-hydroxybutyrate (BHB)) in the liver leading to ketosis (Oetzel 2004). Ketosis is not only linked to lower milk production, but also affects milk quality by inducing changes in milk fat content (Duffield *et al.* 2009; Zhang *et al.* 2019). Zhang *et al.* (2020) reported that a variety of variables including BHB control the synthesis of fatty acids. Thus, understanding the mechanisms controlling alterations in lipid accumulation caused by BHB in bovine mammary epithelial cells (BMECs) may offer effective strategies for sustaining bovine mammary gland health and milk production.

Long chain fatty acyl-CoA ligase 4 (ACSL4) is a member of the acyl-CoA synthetases (ACS) family, which converts FAs to fatty acyl-CoA esters (Zhu *et al.* 2013). In human and rat liver, ACSL4 expression levels are correlated with formation of triglycerides and lipid content (Kotronen *et al.* 2009; Tuohetahuntila *et al.* 2015). Despite the fact that ACSL4 activation produces acyl-CoA and channels FAs for oxidation or lipid biosynthesis, the connection between ACSL4 and aberrant lipid metabolism is still unknown (Chen *et al.* 2021). Furthermore, it is unknown if ACSL4 affects other lipid metabolism-related enzymes.

In bovine mammary epithelial cells, regulatory elements and enzymes including acetyl-CoA carboxylase (ACC), fatty acid synthase (FASN), stearoyl-CoA desaturase (SCD) and sterol regulatory element-binding protein family (SREBPs) are regarded as the major enzymes involved in the FA synthesis and FA uptake (Zhang *et al.* 2020; Liu *et al.* 2021; Li *et al.* 2023). Functionally, the activation of ACSL4 resulted in higher levels of monounsaturated and polyunsaturated fatty acids in pig intramuscular adipocytes (Ren *et al.* 2022), but (at least in hepatocytes) silencing of ACSL4 enhanced PPARα and PGC-1α activity in mice (Duan *et al.* 2022). The latter are central regulators of mitochondrial fatty acid β-oxidation by controlling the levels of several genes including CPT1A (Jia *et al.* 2023; Li *et al.* 2023). In fact, at least in nonruminants, the PGC1αPPARα axis boosts the ability for mitochondrial fatty acid oxidation (Finck *et al.* 2006). Whether ACSL4 impacts fatty acid metabolism in BMECs is unknown. However, unlike other ACSLs, the fact that ACSL4 decreased markedly in bovine mammary tissue after parturition underscores the different roles that these enzymes play in the context of fatty acid metabolism (Bionaz and Loor 2008a). Clearly, a better understanding of fatty acid metabolism in the mammary gland could be achieved by examining some of the key regulators of lipid metabolism including fatty acid oxidation, particularly during times when the supply of BHB to the gland increases.

Ketosis, common during early lactation, involves high BHB levels. Some BHB reaching the mammary gland is used as a precursor for fatty acid synthesis. It was hypothesized that ACSL4 activation in BMECs would promote fatty acid content and lipid droplet accumulation during early lactation, particularly under elevated BHB levels associated with ketosis. The primary goal of the current investigation was to use mammary gland biopsies from ketotic cows and immortalized bovine mammary epithelial cells (MAC-T) challenged with BHB to gather preliminary data on the function of ACSL4 in the context of increased fatty acid content and lipid droplet accumulation. This work offers a theoretical foundation for understanding the molecular processes underlying high milk fat concentrations in ketotic cows and offers a rationale for regulating lipid production in the dairy sector.

2. Materials and methods

2.1. Animals

The experiments were performed at commercial dairy farm in Heilongjiang Province, China. In the daily management of the pasture, lactating multiparous Holstein cows were housed in a free-stall barn. The basic diet composition and nutrient composition of lactating cows are shown in Table 1. The diets were formulated to meet or exceed the requirements of dairy cattle for all nutrients as recommended by the NRC (NASEM 2021). Components of feed were mixed as TMR by TMR SINO-GER mixer (Bvl Inc., Germany) and TMR were fed 3 times per day (at 06:00, 14:00 and 22:00 h) and had free access to feed and water was provided *ad libitum*. All cows were examined by the attending veterinarian during routine medical examinations to determine the absence of co-morbidities.

Thirty-eight Holstein cows during early lactation with

Table 1 Ingredients and chemical composition of lactation diets fed to cows

Ingredient composition[1)]	Content	Nutrition composition[2)]	Contents
Alfalfa hay (%)	10.25	DM (% of TMR)	49.30
Corn silage (%)	28.19	Ash (%)	8.35
Wheat straw (%)	10.25	CP (%)	18.03
Corn germ meal (%)	24.91	NDF (%)	32.19
Soybean meal (%)	7.79	NFC (%)	42.09
Wheat bran (%)	8.71	Crude fiber (%)	12.00
Cottonseed (%)	7.18	Crude fat (%)	3.38
Limestone (%)	1.33	DCAD2 (mEq 100 g^{-1})	20.17
Sodium bicarbonate (%)	0.50	Lys (Met)	2.95:1
Calcium phosphate (%)	0.12	ME (Mcal kg^{-1})	2.65
NaCl (%)	0.30	NE_L (Mcal kg^{-1})	1.71
Magnesium oxide (%)	0.15	NEm (Mcal kg^{-1})	1.71
Vitamin-mineral premix (%)	0.32	NEg (Mcal kg^{-1})	1.12
Total (%)	100.00		

[1)] Provided per kilogram of TMR diet: vitamin A, 2,500 IU; vitamin D_3, 500 IU; vitamin E, 70 IU; Cu (as reagent grade blue copperas), 6.4 mg; Mn (as reagent grade manganese sulfate monohydrate), 15.20 mg; Zn (as reagent grade zinc sulfate heptahydrate), 51.80 mg; I (as feed grade calcium iodate), 0.60 mg; Se (as feed grade sodium selenite), 0.17 mg; Co (as reagent grade cobalt carbonate), 0.09 mg.

[2)] DM, dry matter; TMR, total mixed ration; CP, crude protein; NDF, neutral detergent fiber; NFC, non-fiber carbohydrates; DCAD, dietary anion cation difference (DCAD=(Na^++K^+)–(Cl^-+S^{2-})); ME, metabolizable energy; NE_L, net energy for lactation; NEm, energy for maintainance; NEg, net energy for gain.

comparable number of lactations (median=3, range: 2 to 4) and days in milk (DIM, median=10 d, range: 5 to 21) were selected for blood collection in the tail vein at 04:00 am on the same day. The blood sample collected from each cow was divided into two parts, one blood sample was immediately measured for BHB levels using a blood ketone meter and record the value and the other blood sample was centrifuged at 3,000 r min^{-1} and 4°C to obtain serum samples and stored at –20°C for analyses of glucose content. Serum glucose was measured by a Roche Cobas 6000 c501 automatic biochemical analyzer (Guangzhou150Zhanquan Biotechnology Co., Ltd.). Ketosis was verified using the blood BHB concentration according to our previous reports (Zhang *et al.* 2020). Based on blood BHB levels, 12 cows were selected for mammary biopsy: Six cows with blood BHB levels>2.0 mmol L^{-1} were defined as ketotic, whereas the remaining 6 with BHB levels<0.6 mmol L^{-1} served as the healthy controls. At 04:30 am on the same day, after the blood samples had been taken, 12 cows (DIM, median=13 d, range: 6 to 18) were milked 3 times at 05:00 am, 13:00 pm, and 21:00 pm. The dairy farm used a rotary milking unit to record each milk production (AutoRotor Performer Plus, GEM Inc., Munich, Germany). At the same time, a walkthrough static scale (Pellon Group, Finland) was used every time they left the milking parlor to keep track of cows' body weight. The milk yield and cow weight of 12 cows are recorded after each milking. Statistical milk production is the sum of 3 milkings in one day, and statistical body weight is the average of 3 weighings in one day. The body weight, milk production, serum glucose content and blood BHB level of the 12 cows are shown in Table 2. On the second day at 06:00 am, 12 cows were biopsied for mammary gland tissue.

2.2. Mammary gland tissue biopsy

Percutaneous biopsies were taken from the midpoint of one rear quarter in accordance with published techniques (Bionaz and Loor 2008b). Briefly, intramuscular injection of 2% lidocaine (0.05 mg kg^{-1} BW; 2% Seractal, Bayer, Leverkusen, Germany) was administered, and the mammary gland tissue was cleaned using an iodine tincture and 70% ethanol. To make sure the tissue taken was mammary parenchyma, the mammary capsule was bluntly dissected after the skin incision. As soon as the biopsy tool was removed from the capsule, pressure was given to the entry area to prevent blood clotting beneath the skin. The samples were immediately frozen in liquid nitrogen and kept there until analysis.

2.3. Cell culture

The immortalized bovine MAC-T was purchased from Shanghai chuanqiu Biotechnology Co., Ltd. MAC-T cells were grown in 75-cm^2 cell culture flasks with 10% fetal bovine serum, 100 U mL^{-1} penicillin, and 100 μg mL^{-1} streptomycin added to DMEM/F-12 medium in a 37°C incubator with 5% CO_2. 0.05% trypsin and 0.53 mmol L^{-1} EDTA were used to separate the cells until cell density was 80%, and cells were passaged into fresh cell culture flasks. The cell density was changed to 4×10^5 cells cm^{-2}. Then a 6-well plate was planted with the MAC-T cells solution (2 mL per well). Cells were grown in lactogenic medium for about 24 h before treatments (1 g L^{-1} BSA and 2.5 mg L^{-1} prolactin added to DMEM/F-12 medium) (Kadegowda *et al.* 2009).

2.4. Dose response with BHB and transfections

During the *in vitro* challenge, a BHB sodium salt was used (Sigma-Aldrich, USA). BHB powder was dissolved in distilled water and sterilized by filtering prior to culture. Mammary epithelial cells were serum-starved for 12 h prior to treatments. To select the most appropriate stimulation concentration, cells were grown in a medium devoid of serum containing 0, 0.3, 0.6, 1.2, and 2.4 mmol L^{-1} BHB for 24 h. To select the most appropriate stimulation time, cells were grown in a medium devoid of serum containing 1.2 mmol L^{-1} BHB for 0, 3, 6, 12, 24, and 48 h.

For transient transfections, 12 h prior to the experiment, 4×10^5 cells (6-well plate) were planted, followed by siRNA-Mate transfection reagent using 40 pmol L^{-1} bovine ACSL4 small interfering RNA (siRNA; Shanghai GenePharma Co., Ltd., Shanghai, China) or nontarget siRNA (Shanghai GenePharma Co., Ltd.) in accordance with the manufacturer's instructions. After 24 h, cells received 1.2 mmol L^{-1} BHB treatment for an additional 24 h. The following siACSL4 sequence were used: S (5′–3′): GCUGUAGUUCAUGGGUUAATT; AS (5′–3′): UUAACCCAUGAACUACAGCTT.

The ACSL4 overexpression plasmid pcDNA3.1-ACSL4 (named pcACSL4) was designed and synthesized by Jiangsu Genecefe Biotechnology Co., Ltd., MAC-T cells were cultured in 6-well plate and were transfected with pcDNA3.l plasmid as the control group and pcACSL4 plasmid as the treatment group using Lipofectamine 2000 (11668019, ThermoFisher Scientific, USA) when the cell density reached 70% confluency according to the manufacturer's protocol. Thirty-six hours posttransfection, the cells were exposed to BHB for another 24 h.

2.5. mRNA extraction and quantitative real-time PCR

MAC-T cells' total mRNA was extracted using Trizol in accordance with the manufacturer's instructions (Invitrogen Corporation). Reverse transcriptase M-MLV (RNase H-; RR047A, TaKaRa Biotechnology Co., Ltd.) was used to convert cDNA from 1 μg of total RNA. The quantitative real-

Table 2 Basic performance and energy balance biomarkers in healthy cows and cows with ketosis

Item	Ketosis (*n*=6)		Healthy (*n*=6)		*P*-value
	Median	Interquartile range	Median	Interquartile range	
Body weight (kg)	632	626, 636	653	637, 657	0.0341
Milk production (kg d^{-1})	25.6	24.9, 26.0	32.1	31.0, 32.9	<0.0001
Serum glucose (mmol L^{-1})	2.25	2.00, 2.48	3.99	3.87, 4.13	<0.0001
β-Hydroxybutyrate (mmol L^{-1})	2.25	2.13, 2.60	0.250	0.200, 0.300	<0.0001

time (qRT)-PCR reaction system (20 μL) was as follows: 2 μL of cDNA, 1 μmol L^{-1} of each primer, 10 μL of FastStart Universal SYBR Green Master (F. Hoffmann-La Roche AG, Basel, Switzerland) and sterile water; qRT-PCR reaction conditions were: starting temperature of 95°C for 3 min, followed by 95°C for 10 s and 58°C for 30 s, a total of 40 cycles. Calculated mRNA abundance levels were normalized to β-actin (ACTB) using the $2^{-\Delta\Delta C_T}$ method. Evaluated target genes (*FASN*, *ACACA*, *ACSL4*, *SREBP1*, *DGAT1*, *DGAT2*, *SCD1*, *PPARα*, *PGC-1α*, *CPT1A*) are reported in Appendix A.

2.6. Protein extraction and Western blotting

RIPA buffer (Beyotime Biotechnology, China) containing protease inhibitor was used to lyse MAC-T cells followed by 30 min on ice and 5 min at 4°C and 14,000×g of centrifugation. Aliquots of 30 g of total protein were loaded with known molecular weight markers onto 10% SDS polyacrylamide gels (Solarbio Life Sciences, China). The protein was then electro-transferred to the polyvinylidene difluoride membranes (Millipore Corp., Billerica, MA). The polyvinylidene difluoride membranes were blocked in a tris-buffered saline solution (50 mmol L^{-1} Tris, pH=7.6, 150 mmol L^{-1} NaCl, and 0.1% Tween 20) for 1 h at room temperature. The blocked membranes were incubated at 4°C for the whole night with specific antibodies for FASN (1:1,000, 3180; cell signaling), ACACA (1:1,000, 3662; cell signaling, Danvers, MA), ACSL4 (1:1,000, A6826, Abclonal), SREBP1 (1:1,000, NB100–2215; Novus Biologicals, Littleton, CO), DGAT1 (1:1,000, ab122924, Abcam), PPARγ (1:1,000, A0270, Abclonal), DGAT2 (1:2,000, A13890, ABclonal), SCD1 (1:1,000, 2794; cell signaling), PPARα (1:1,000, bs-3614R, Bioss), PGC-1α (1:1,000, AF5395, Affinity), CPT1A (1 μg mL^{-1}, ab83862, Abcam), and β-actin (internal control; 1:1,000, sc-47778; Santa Cruz Biotechnology). The membranes were then incubated with secondary antibodies that were HRP-conjugated (3:5,000; Beyotime Biotechnology) for 45 min at room temperature. Protein abundance signals were detected with a protein imager (ProteinSimple, San Jose, CA).

2.7. Immunofluorescence of cytokeratin 18

At a density of 1×10^5 cells/well, MAC-T cells were seeded on sterile glass coverslips and then given a gentle PBS wash. The cells were fixed with pre-cooled methanol. Three times for 5 min each, coverslips were washed in PBS. Blocking buffer (5% goat serum (Sigma) in PBS) was applied to the cells and left on them for 1 h at room temperature. Cells were then incubated with a 1:200 dilution of FITC anti-cytokeratin 18 (10830-1-AP, Proteintech, China) for 1 h. The cells were given 3 times for 5 min PBS rinses before being exposed to Hoechst (Beyotime Biotechnology) for 8 min at room temperature and in the dark. After that, the laser confocal microscope was used to measure fluorescence after 3 times with PBS washes of the cells (LSM 5 PASCAL, Zeiss, Oberkochen, Germany).

2.8. Lipid droplet fluorescence assay

After removal of culture fluid, MAC-T cells were washed 3 times with PBS before being fixed for 30 min with 4% paraformaldehyde. Cell staining was done with BODIPY 493/503 (Invitrogen Corporation, USA). Afterwards, in the dark, PBS was used to clean the cells 3 times. The nucleus was stained with Hoechst for 8 min at room temperature. (Beyotime Biotechnology). The fluorescence was measured with a laser confocal microscope (LSM 5 PASCAL, Zeiss, Oberkochen, Germany).

2.9. Mitochondrial membrane potential fluorescence assay

After treatment, MAC-T cells were grown in 12-well plates and stained in accordance with the manufacturer's instructions. In brief, JC-1 (Beyotime Biotechnology) dye working solution was added in the treated cells and incubated at 37°C for 10 min. The staining working solution was removed and the excess probe washed away. A laser confocal microscope was used to examine the JC-1 staining signal (LSM 5 PASCAL, Zeiss, Oberkochen, Germany).

2.10. Flow cytometry

To ascertain intracellular alterations in reactive oxygen species (ROS), a ROS test kit (Beyotime Biotechnology) was employed. A total of 10 μmol L^{-1} carboxy-2′,7′-dichloro-dihydrofluorescein diacetate probe was treated with 1×10^5 cells for 30 min at 37°C. Using a Beckman CytoFLEX flow cytometer, fluorescence was recorded at 488 nm (excitation) and 525 nm (emission) (Beckman Coulter, Brea, CA).

2.11. Statistical analysis

Data are mean±SE. All analysis was performed with GraphPad Prism Program (Prism 9.0; GraphPad software, San Diego, CA) or SPSS 26.0 software (IBM, Chicago, IL). *In vivo* experiments, individual cow (n=6) as the experimental units, while *in vitro* experiments, each cell culture-well (6-well per plate) (n=3) as the experimental unit. Prior to analysis, all data underwent tests for normality and homogeneity of variance and residuals using the Shapiro. Wilk and Levene tests, respectively. Basic characteristics of the cows with a skewed distribution underwent a nonparametric statistical analysis using the Wilcoxon test (Zhu *et al.* 2019). Basic characteristics of dairy cows are presented as the median and interquartile range. The comparison of data between healthy and ketosis cows was conducted using the *t*-test. Dose and time-dependent effects was conducted using one-way ANOVA with subsequent orthogonal comparisons (unequally spaced) were applied for linear and quadratic responses. In evaluating the effects of ACSL4 (silence or overexpression experiment) under BHB stimulation conditions, two-way ANOVA method was used, and the statistical model included BHB treatment, ACSL4 silence/ overexpression and their interaction. Differences among means were tested by the least significant difference (LSD) method. Statistical significance was set at P<0.05.

3. Results

3.1. mRNA and protein abundance in healthy cows or cows with ketosis

Relative mRNA and protein abundance in mammary tissue for fatty acid synthesis-related genes showed that *FASN*,

ACACA, *ACSL4*, *SREBP1*, *DGAT1*, *PPARγ*, *DGAT2*, and *SCD1* were greater (P<0.01; Fig. 1) in cows with ketosis compared with the healthy group. In contrast, mRNA and protein abundance of fatty acid oxidation-related-CPT1A was lower (P<0.01; Fig. 1) in cows with ketosis.

3.2. BHB increased fatty acid content

Cytokeratin 18 (CK-18) confirmed the epithelial nature of the MAC-T (Fig. 2-A). The mRNA and protein abundance of FASN, ACACA, ACSL4 and CPT1A were affected (Fig. 2, P≤0.0002) by treatment with different dose of BHB. With increasing BHB dose, the mRNA expression of *FASN* increased linearly (P<0.0001) and quadratically (P=0.0118), with 1.2 or 2.4 mmol L^{-1} BHB (P<0.05, Fig. 2-B) higher mRNA expression than those from the 0 mmol L^{-1} group. Compared with the 0 mmol L^{-1} group, mRNA expression of *ACACA* and *ACSL4* reached their highest level at 1.2 mmol L^{-1} BHBA (P<0.05), followed by a decrease at subsequent concentration points, displaying linear (ACACA: P=0.0002 and *ACSL4*: P<0.0001) and quadratic (ACACA: P=0.0156 and *ACSL4*: P=0.0400) trends (Fig. 2-C and D); the mRNA expression of *CPT1A* had linear decreases (P<0.0001), and was lower at the 1.2 and 2.4 mmol L^{-1} BHB (P<0.05, Fig. 2-E) than that of 0 mmol L^{-1} group. Compared with the 0 mmol L^{-1} group, protein abundance of FASN reaching their highest level at 2.4 mmol L^{-1} BHB (P<0.05), displaying linear trends (P<0.0001, Fig. 2-F and G); protein abundance of ACACA and ACSL4, had both linear (ACACA: P<0.0001 and ACSL4: P=0.0021) and quadratic (ACACA: P<0.0001 and ACSL4: P=0.0079) increases, with peaks at 0.6 (P<0.05) and 1.2 mmol L^{-1} (P<0.05), respectively, followed by a decrease at higher dose points (Fig. 2-F, H and I); protein abundance of CPT1A had linear decreases (P<0.0001), and was lower at 2.4 mmol L^{-1} BHB (P<0.05, Fig. 2-F and J).

The mRNA and protein abundance of FASN, ACACA, ACSL4 and CPT1A were all affected (Fig. 3, P≤0.0084) by treatment for different times with BHB. Compared with the 0 h group, mRNA expression of *FASN*, *ACACA* and *ACSL4*, had both linear (*FASN*: P=0.0044, *ACACA*: P<0.0001 and ACSL4: P=0.0276) and quadratic (FASN: P=0.0009, ACACA: P=0.0080 and ACSL4: P=0.0020) increases, with highest mRNA expression at 24 h (P<0.05), followed by a decrease at later time points (Fig. 3-A–C); The mRNA expression of *CPT1A* was decreased gradually over treatment time, displaying linear trends (P<0.0001, Fig. 3-D). Compared with the 0 h group, protein abundance of FASN had linear

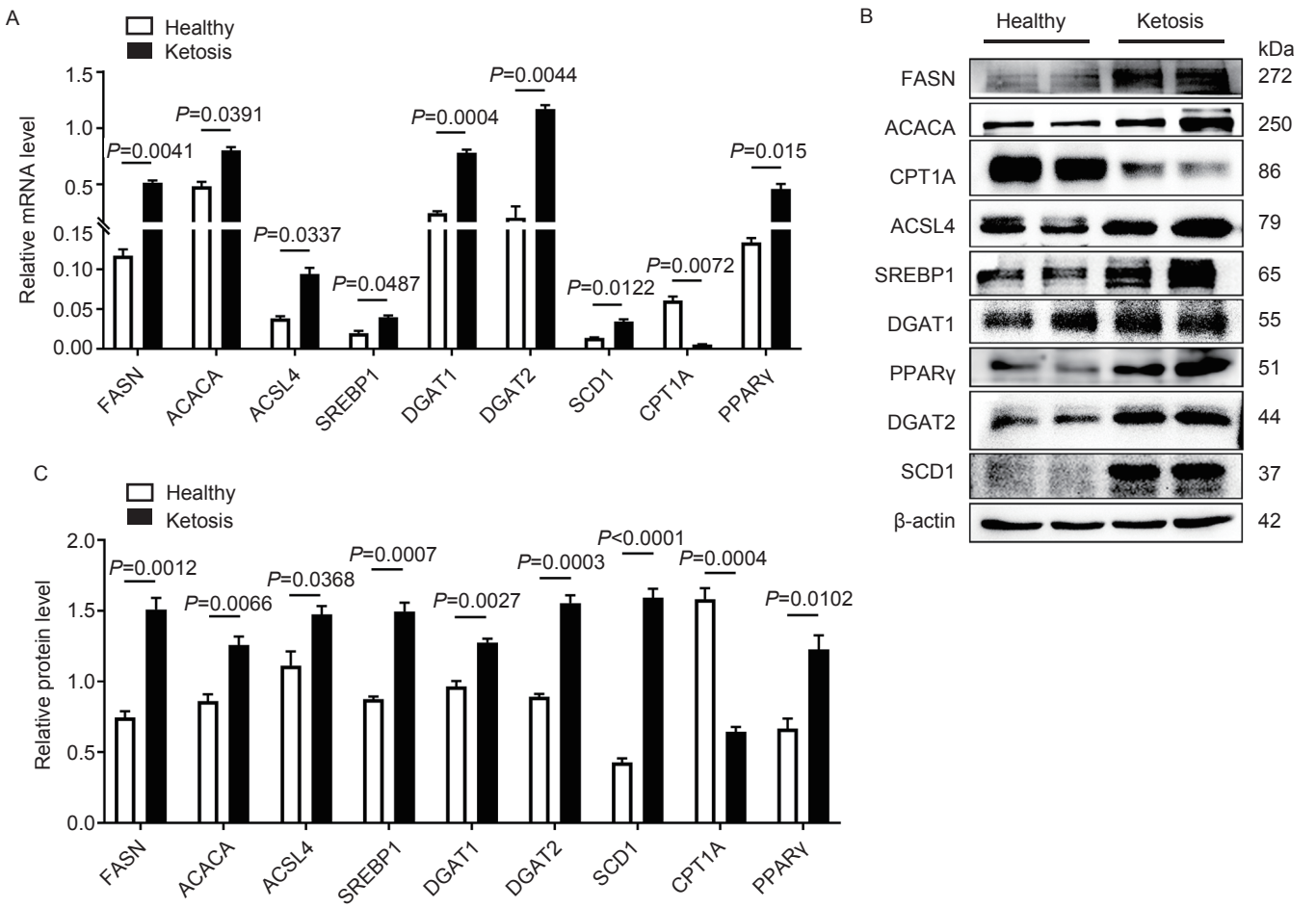


Fig. 1 Measurement of mammary tissue mRNA and protein expression in healthy cows and ketosis cows. Panel (A) relative mRNA abundance of *FASN*, *ACACA*, *ACSL4*, *SREBP1*, *DGAT1*, *DGAT2*, *SCD1*, *PPARγ*, and *CPT1A* (n=6). B, Western blots of FASN, ACACA, ACSL4, SREBP1, DGAT1, PPARγ, DGAT2, SCD1, and CPT1A (n=6). C, relative protein abundance of FASN, ACACA, ACSL4, SREBP1, DGAT1, PPARγ, DGAT2, SCD1, and CPT1A (n=6). Data are mean±SE.

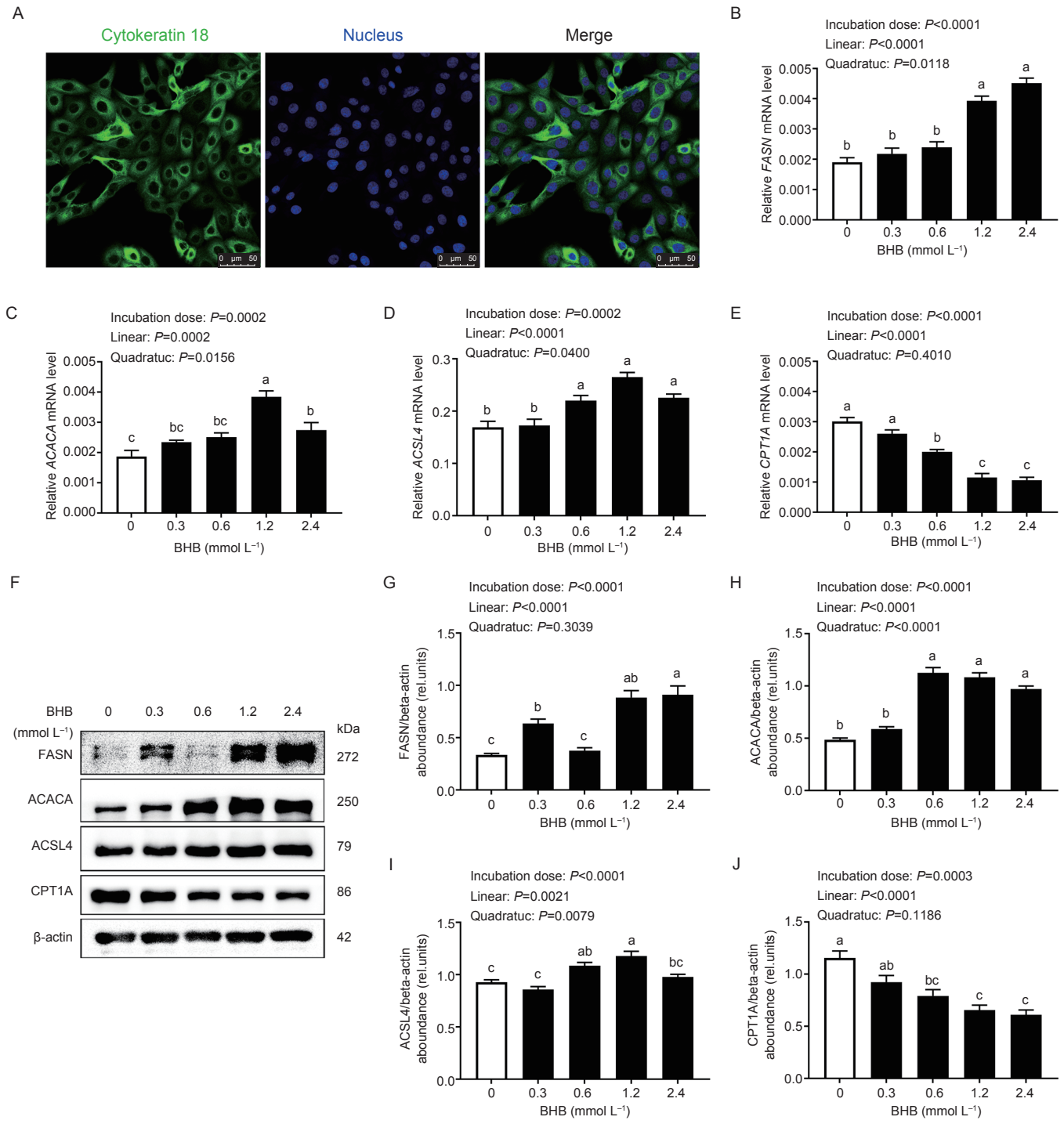


Fig. 2 Effects of different concentrations of BHB on FASN, ACACA, ACSL4, and CPT1A mRNA or protein expression in MAC-T cells. Cells were treated with 0, 0.3, 0.6, 1.2 or 2.4 mmol L^{-1} BHB for 24 h. A, identification of cytokeratin-18 immunofluorescence. B–E, relative levels of mRNA for *FASN*, *ACACA*, *ACSL4*, and *CPT1A* (n=3). F, Western blots of FASN, ACACA, ACSL4, and CPT1A (n=3). G–I, relative abundance protein content of FASN, ACACA, ACSL4, and CPT1A (n=3). BHB, β-hydroxybutyrate; FASN, fatty acid synthase; ACSL4, long chain fatty acyl-CoA ligase 4; MAC-T, mammary epithelial cell line; rel. units, relative units. Data are mean±SE. Different superscript lowercase letters in bar charts represent significant difference (P<0.05).

increases (P<0.0001), with peaks at 48 h post BHB treatment (Fig. 3-E and F); protein abundance of ACACA, had both linear (P<0.0001) and quadratic (P<0.0001) increases, with highest level at 24 h (P<0.05), followed by a decrease at later time points (Fig. 3-E and G). With increasing BHB treatment time, the protein abundance of ACSL4 increased linearly (P=0.0218). 24 h BHB treatment (P<0.05, Fig. 3-E and H) had higher protein abundance than those from the 0 h group; protein abundance of CPT1A was lower at 24 h post BHB treatment (P<0.05), displaying linear (P=0.0003) and

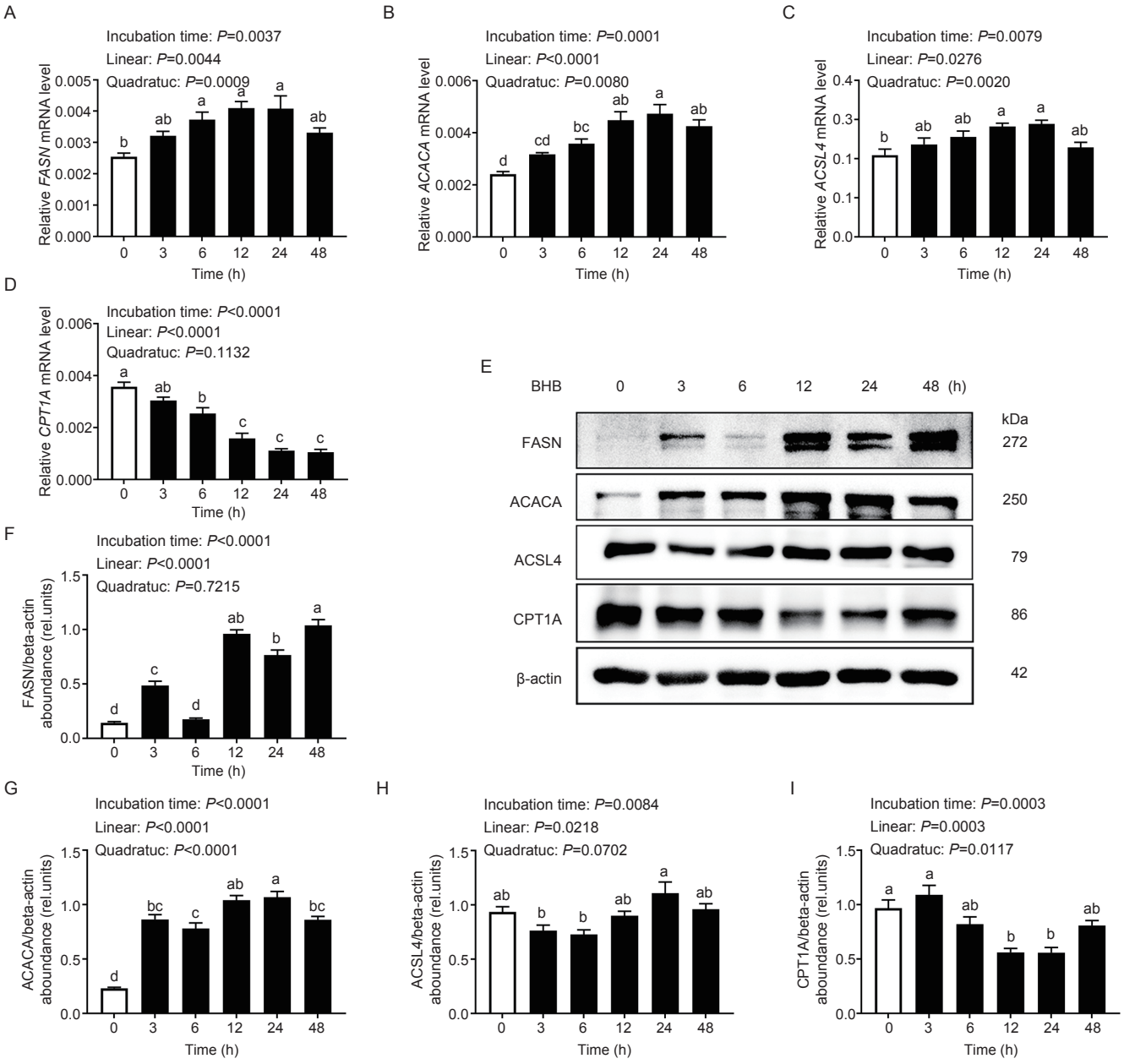


Fig. 3 Effects of different incubation times with BHB on FASN, ACACA, ACSL4, and CPT1A mRNA or protein expression in MAC-T cells. Cells were stimulated with 1.2 mmol L^{-1} BHB for 0, 3, 6, 12, 24 or 48 h respectively. A–D, relative mRNA abundance of *FASN*, *ACACA*, *ACSL4*, and *CPT1A* (n=3). E, Western blots of FASN, ACACA, ACSL4, and CPT1A (n=3). F–I, relative protein abundance of FASN, ACACA, ACSL4, and CPT1A (n=3). BHB, β-hydroxybutyrate; FASN, fatty acid synthase; ACSL4, long chain fatty acyl-CoA ligase 4; rel. units, relative units. Data are mean±SE. Different superscript lowercase letters in bar charts represent significant difference (P<0.05).

quadratic (P=0.0117) trends (Fig. 3-E and I).

3.3. Effect of silencing ACSL4 on fatty acid content

Interaction effect of BHB treatment and silencing ACSL4 was found on mRNA expression of *FASN* (P=0.0011), *ACACA* (P=0.0199), *ACSL4* (P=0.0053), *DGAT1* (P=0.0015), *DGAT2* (P=0.0073) and *PPARγ* (P=0.0031), and protein abundance of FASN (P=0.0008), ACACA (P=0.0036), PPARγ (P=0.0188), DGAT2 (P=0.0386) and SCD1 (P=0.0051), but not observed on mRNA expression of *SCD1* and *SREBP1*, and protein abundance of ACSL4, SREBP1 and DGAT1 (Fig. 4). Compared with the siControl, mRNA expression of *FASN*, *ACACA*, *ACSL4*, *DGAT1*, *DGAT2* and *PPARγ*, and protein abundance of FASN, ACACA, PPARγ and SCD1 were greater (P<0.05) in siControl+BHB (Fig. 4-A–C, F–K, and O–Q). The mRNA expression of *FASN*, *ACSL4*, *DGAT1*, *DGAT2* and *PPARγ* were not affect (Fig. 4-A, C and F–H) in siACSL4+BHB compared with the siACSL4, but influenced (P<0.05) mRNA expression of *ACACA* and protein abundance of FASN, ACACA, PPARγ, DGAT2, and SCD1 (Fig. 4-B, J, K and O–Q).

Silencing ACSL4 did not affect protein expression levels of DGAT1 (Fig. 4-N), but influenced (P≤0.0255) mRNA expression levels of *SCD1* and *SREBP1*, and protein

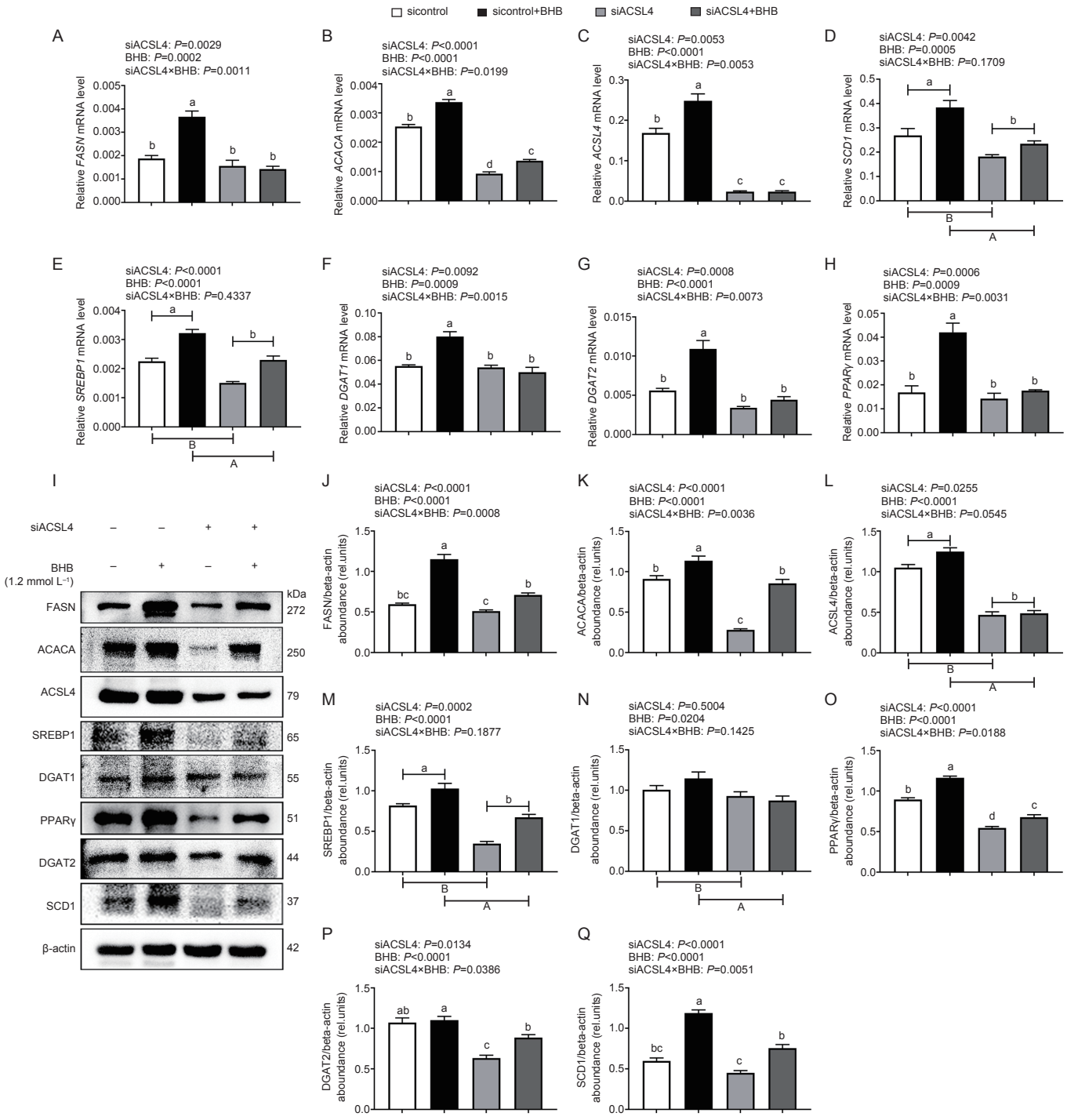


Fig. 4 Effect of silencing ACSL4 on lipid synthesis in MAC-T cells. MAC-T cells were treated with ACSL4 transient transfection (siACSL4) for 24 h, and incubated with 1.2 mmol L^{-1} BHBA for another 24 h. A–H, relative mRNA abundance of *FASN*, *ACACA*, *ACSL4*, *SREBP1*, *DGAT1*, *PPARγ*, *DGAT2*, and *SCD1* (n=3). I, Western blots of FASN, ACACA, ACSL4, SREBP1, DGAT1, PPARγ, DGAT2, and SCD1 (n=3). J–Q, relative protein abundance of FASN, ACACA, ACSL4, SREBP1, DGAT1, PPARγ, DGAT2, and SCD1 (n=3). Data are mean±SE. Different lowercase letters in single bars (individual treatments) represent significant difference (P<0.05) determined by their interaction. Different lowercase letters in double bars means significant differences at P<0.05 between non-silencing ACSL4 and silencing ACSL4 as determined by a main effect of silencing ACSL4. BHB, β-hydroxybutyrate; FASN, fatty acid synthase; ACSL4, long chain fatty acyl-CoA ligase 4; MAC-T, mammary epithelial cell line; rel. units, relative units. Different capital letters in double bars means significant differences at P<0.05 between non-BHB treatment and BHB treatment as determined by a main effect of BHB treatment.

expression levels of ACSL4 and SREBP1 (Fig. 4-D, E, L and M). Added BHB treatment did influenced (P≤0.0204) mRNA expression levels of *SCD1* and *SREBP1*, and protein expression levels of ACSL4, SREBP1 and DGAT1 (Fig. 4-D, E and L–N). Compared to non-silencing ACSL4, silencing ACSL4 reduces the mRNA expression of *SCD1* and *SREBP1* (P≤0.0042, Fig. 4-D and E), and protein abundance of ACSL4 and SREBP1 (P≤0.0255, Fig. 4-L and M). Compared to

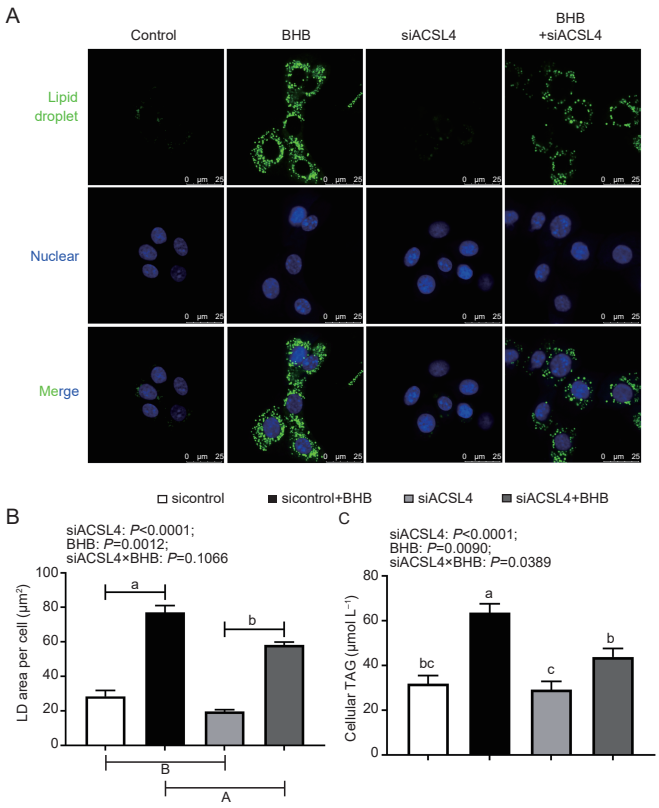


Fig. 5 Effect of silencing ACSL4 on lipid droplet immunofluorescence and triglyceride (TAG) concentration in MAC-T cells. Cells were treated with ACSL4 transient transfection (siACSL4) for 24 h, and incubated with 1.2 mmol L^{-1} BHBA for another 24 h. A, immunofluorescence results of lipid droplets (n=3). B, LD area per cell (n=3). C, TAG content in MAC-T cells (n=3). Data are mean±SE. Different lowercase letters in single bars (individual treatments) represent significant difference (P<0.05) determined by their interaction. Different lowercase letters in double bars means significant differences at P<0.05 between non-silencing ACSL4 and silencing ACSL4 as determined by a main effect of silencing ACSL4. Different capital letters in double bars means significant differences at P<0.05 between non-BHB treatment and BHB treatment as determined by a main effect of BHB treatment. BHB, β-hydroxybutyrate; ACSL4, long chain fatty acyl-CoA ligase 4; MAC-T, mammary epithelial cell line.

non-BHB treatment, BHB treatment increased the mRNA expression of *SCD1* and *SREBP1* (P≤0.0005, Fig. 4-D and E), and protein abundance of ACSL4, SREBP1 and DGAT1 (P≤0.0204, Fig. 4-L–N).

3.4. Effect of silencing ACSL4 on lipid droplet accumulation

There was no interaction effect of BHB treatment and silencing ACSL4 on LD area per cell, but found on cellular TAG (P=0.0389, Fig. 5). Compared with the sicontrol, triacylglycerol (TAG) level was greater (P<0.05) in sicontrol+BHB (Fig. 5-C). The content of TAG was greater (P<0.05) in siACSL4+BHB compared with the siACSL4. BHB treatment (P=0.0012) and silencing ACSL4 affected (P<0.0001) affected LD area per cell (Fig. 5-B), respectively. Compared to non-silencing ACSL4, silencing ACSL4 reduces the LD area per cell (P<0.0001, Fig. 5-B). Compared to non-BHB treatment, BHB treatment increased the LD area per cell (P=0.0012, Fig. 5-B).

3.5. Effect of silencing ACSL4 on fatty acid oxidation and mitochondrial function

Interaction effect of BHB treatment and silencing ACSL4 was found on mRNA expression of *CPT1A* (P=0.0257), protein abundance of PPARα (P=0.0309), PGC-1α (P=0.0117) and CPT1A (P=0.0007), mitochondrial membrane potential (MMP, P<0.0001), and ROS production (P=0.0006) (Fig. 6-C–K), but not observed on mRNA expression of *PPARα* and *PGC-1α* (Fig. 6-A and B). Compared with the siControl, mRNA expression of *CPT1A*, protein abundance of PPARα, PGC-1α and CPT1A was lower (P<0.05) in sicontrol+BHB (Fig. 6-C–G), and mitochondrial membrane potential, and ROS production were greater (P<0.05) in siControl+BHB (Fig. 6-H–K). The protein abundance of PGC-1α and ROS level were not affect (Fig. 6-F and K) in siACSL4+BHB compared with the siACSL4, but influenced (P<0.05) mRNA expression of *CPT1A*, protein abundance of PPARα and CPT1A, and mitochondrial membrane potential (Fig. 6-C, E, G and I).

Silencing ACSL4 influenced (P≤0.0013) mRNA expression levels of *PPARα* and *PGC-1α* (Fig. 6-A and B). Added BHB treatment did influence (P≤0.0078) mRNA expression levels of *PPARα* and *PGC-1α* (Fig. 6-A and B). Compared to non-silencing ACSL4, silencing ACSL4 increased the mRNA expression of *PPARα* and *PGC-1α* (P≤0.0013, Fig. 6-A and B). Compared to non-BHB treatment, BHB treatment decreased the mRNA expression of *PPARα* and *PGC-1α* (P≤0.0078, Fig. 6-A and B).

3.6. ACSL4 exacerbate BHB-induced fatty acid content and lipid droplet accumulation in MAC-T cells

There was no interaction effect of BHB treatment and ACSL4 overexpression on protein abundance of FASN, CPT1A, SREBP1 and DGAT2 except for protein abundance of ACACA (P=0.0184), ACSL4 (P=0.0315), DGAT1 (P=0.0198), PPARγ (P=0.0001) and SCD1 (P=0.0017), LD area per cell (P<0.0001), and cellular TAG (P<0.0001, Fig. 7). Compared with the pcDNA, protein abundance of ACACA, ACSL4, DGAT1, PPARγ and SCD1, LD area per cell, and cellular TAG were greater (P<0.05) in pcDNA+BHB (Fig. 7-C, E, G, H, and J–M). The protein abundance of ACACA, ACSL4, DGAT1, PPARγ and SCD1, LD area per cell, and cellular TAG were no affect (Fig. 7-C, E, G, H, and J–M) in pcACSL4+BHB compared with the pcACSL4.

ACSL4 overexpression influenced (P≤0.0456) protein abundance of FASN, CPT1A, SREBP1 and DGAT2. Added BHB treatment did influence (P≤0.006) protein abundance of FASN, CPT1A, SREBP1 and DGAT2 (Fig. 7-B, D, F and I). Compared to non-overexpression of ACSL4, overexpression of ACSL4 increased protein abundance of FASN, SREBP1 and DGAT2 (P≤0.0456, Fig. 7-B, F and I), and decreased protein abundance of CPT1A (P=0.0063) (Fig. 7-D). Compared to non-BHB treatment, BHB treatment increased the protein abundance of FASN, SREBP1 and DGAT2 (P≤0.0065, Fig. 7-B, F and I), and decreased protein abundance of CPT1A (P=0.0031) (Fig. 7-D).

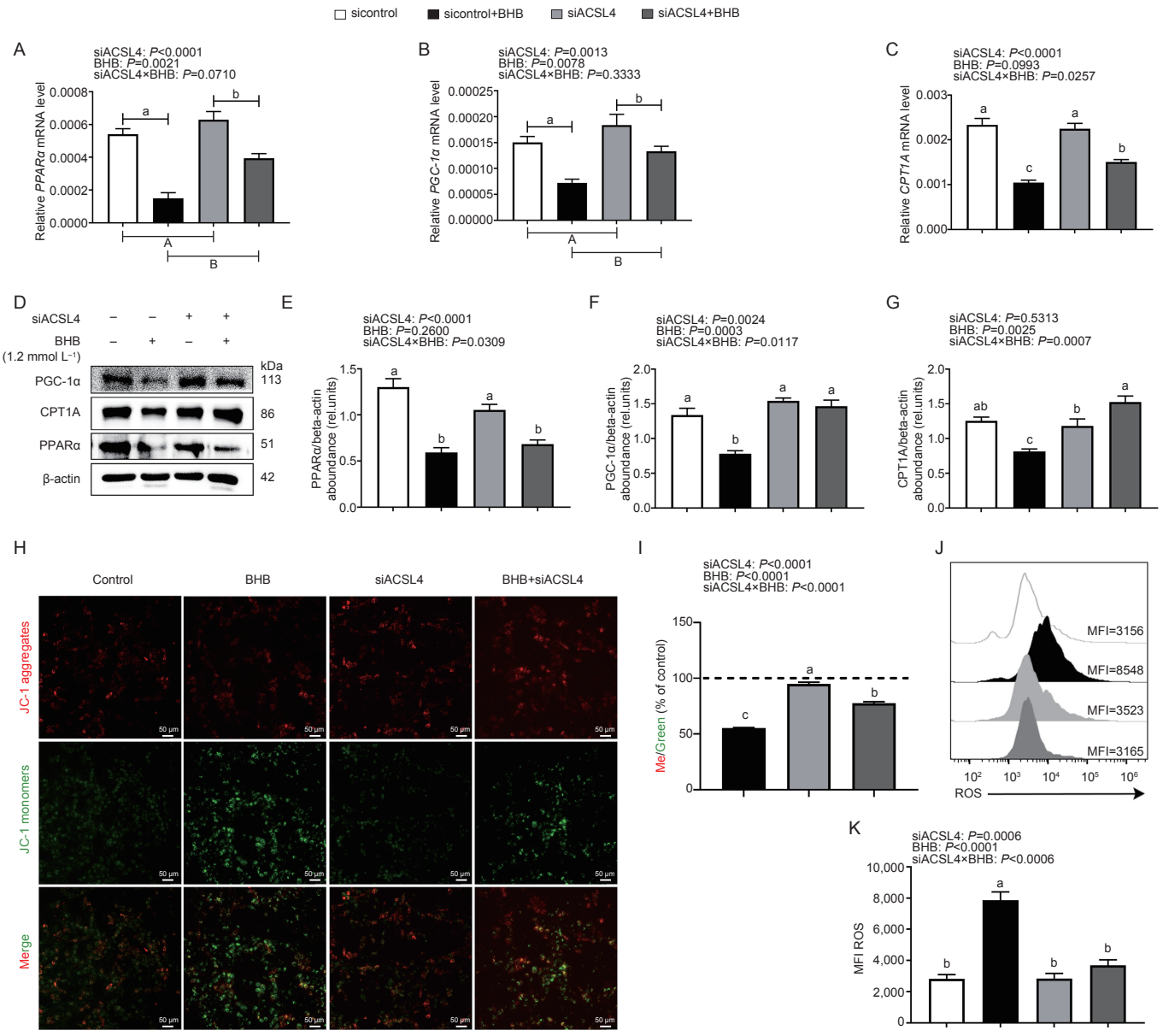


Fig. 6 The effect of silencing ACSL4 on fatty acid oxidation, mitochondrial membrane potential (MMP), and reactive oxygen species (ROS) in MAC-T cells. Cells were treated with ACSL4 transient transfection (siACSL4) for 24 h, and incubated with 1.2 mmol L^{-1} BHBA for another 24 h. A–C, relative mRNA abundance of *PPARα*, *PGC-1α*, and *CPT1A*. D, Western blots of PPARα, PGC-1α, and CPT1A. E–G, relative protein abundance of PPARα, PGC-1α, and CPT1A. H–I, MMP staining in MAC-T cells. J–K, the level of ROS was analyzed by flow cytometry. BHB, β-hydroxybutyrate; ACSL4, long chain fatty acyl-CoA ligase 4; MAC-T, mammary epithelial cell line; rel. units, relative units. Data are mean±SE (*n*=3). Different lowercase letters in single bars (individual treatments) represent significant difference ($P<0.05$) determined by their interaction. Different lowercase letters in double bars means significant differences at $P<0.05$ between non-silencing ACSL4 and silencing ACSL4 as determined by a main effect of silencing ACSL4. Different capital letters in double bars means significant differences at $P<0.05$ between non-BHB treatment and BHB treatment as determined by a main effect of BHB treatment.

4. Discussion

The results from the current study show that ketosis significantly increased mRNA expression levels of *FASN*, *ACACA*, *ACSL4*, *SCD1*, *SREBP1*, *DGAT1*, *DGAT2* and *PPARγ*, and their corresponding protein abundance, and remarkably reduced the expression of *CPT1A* mRNA and protein in mammary gland tissue of dairy cows. Further *in vitro* experiments revealed that BHB significantly increased mRNA expression levels of *FASN*, *ACACA*, *ACSL4*, *SCD1*, *SREBP1*, *DGAT1*, *DGAT2* and *PPARγ*, and their corresponding protein abundance, LD area per cell, TAG level, MMP, and ROS production, and remarkably reduced *PPARα*, *PGC-1α* and *CPT1A*, and their corresponding protein abundance. However, silencing ACSL4 significantly decreased mRNA expression levels of *FASN*, *ACACA*, *ACSL4*, *SCD1*, *SREBP1*, *DGAT1*, *DGAT2* and *PPARγ*, and protein abundance of FASN, ACACA, ACSL4, SCD1, SREBP1, DGAT2 and PPARγ, LD area per cell, TAG level, MMP, and ROS production in

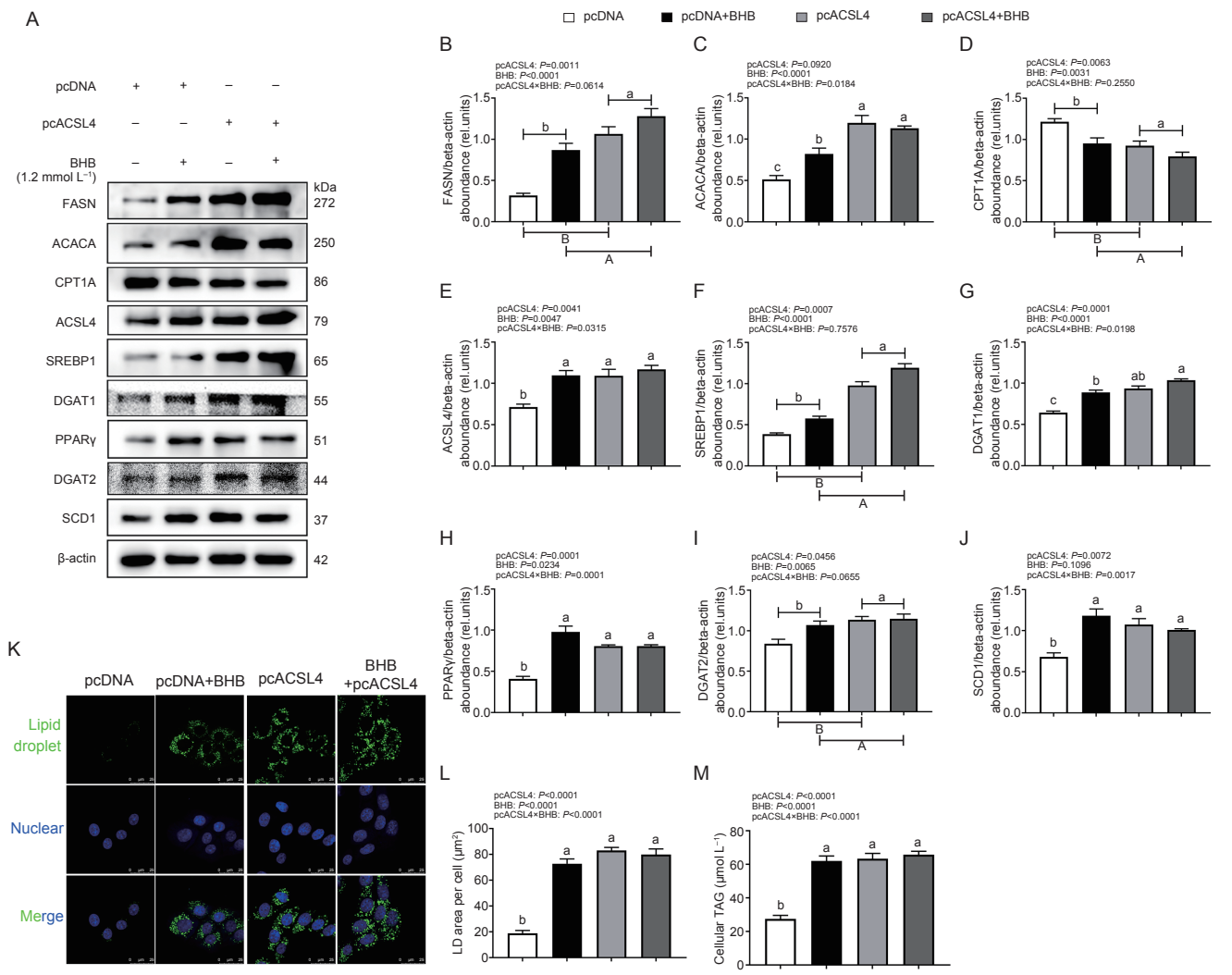


Fig. 7 The effect of overexpression ACSL4 on lipid metabolism in MAC-T cells. Cells were transfected with pcDNA3.1 or pcACSL4 overexpression plasmid by lipofectamine 2000 for 36 h followed by BHB for another 24 h. A, Western blots of FASN, ACACA, CPT1A, ACSL4, SREBP1, DGAT1, PPARγ, DGAT2, and SCD1. B–J, relative protein abundance of FASN, ACACA, CPT1A, ACSL4, SREBP1, DGAT1, PPARγ, DGAT2, and SCD1. K, immunofluorescence results of lipid droplets. L, LD area per cell (n=3). M, TAG content in MAC-T cells. BHB, β-hydroxybutyrate; ACSL4, long chain fatty acyl-CoA ligase 4; MAC-T, mammary epithelial cell line; rel. units, relative units. Data are mean±SE (n=3). Different lowercase letters in single bars (individual treatments) represent significant difference (P<0.05) determined by their interaction. Different lowercase letters in double bars means significant differences at P<0.05 between non-ACSL4 overexpression and ACSL4 overexpression as determined by a main effect of ACSL4 overexpression. Different capital letters in double bars means significant differences at P<0.05 between non-BHB treatment and BHB treatment as determined by a main effect of BHB treatment.

BMECs. In contrast, overexpression ACSL4 significantly increased FASN, ACACA, ACSL4, SREBP1, DGAT1, PPARγ, DGAT2 and SCD1, LD area per cell, and TAG level, and remarkably reduced CPT1A protein abundance. The above results suggest that ACSL4 activation in BMECs would be likely to increase fatty acid content and lipid droplet accumulation during early lactation, especially when BHB levels are elevated due to ketosis, which supports our hypothesis. These findings have not been reported before, and thus provide a scientific foundation for targeting ACSL4 to reduce abnormal fatty acid metabolism in the BMECs of ketotic cows, thereby ensuring the health of BMECs.

Dairy cows frequently experience NEB around parturition, which causes lipid mobilization and results in high circulation of BHB (Bauman and Griinari 2000; Loor *et al.* 2013). Under those conditions, BHB can serve as a precursor for fatty acid synthesis (Duffield *et al.* 2009; Zhang *et al.* 2020). Fatty acid synthesis and the absorption of circulating fatty acids both contribute to lipid droplet accumulation (Steenson *et al.* 2020). Recent studies with mice, pigs and humans reported that ACSL4 is the major protein controlling the fate of fatty acids for lipid droplet accumulation (Chen *et al.* 2021; Duan *et al.* 2022; Ren *et al.* 2022). Although there may be variations among species, the regulatory role of ACSL4 in fatty acid metabolism is well-established. Contrary to the documented relationship between NEFA and synthesis of fatty acids (Sun *et al.* 2019), the biological response of bovine mammary epithelial cells to high BHB concentrations is poorly understood. Further, mechanisms of ACSL4 on fatty acid content and metabolism in bovine mammary gland are

still unclear. Thus, the current study assessed characteristics of ACSL4 and related pathways that coordinate fatty acid content and lipid droplet accumulation in bovine mammary gland using a ketotic cow model. Furthermore, immortalized bovine mammary epithelial (MAC-T) cells were used to study more directly the regulation of ACSL4.

The markedly greater levels of SREBP1, ACACA, FASN, PPARγ, and ACSL4, and significantly lower levels of CPT1A in ketotic cows was consistent with a previous study demonstrating that attenuation of fatty acid oxidation and increased fatty acid content and lipid droplet accumulation in mammary gland from ketotic cows (Fan *et al.* 2020; Zhang *et al.* 2020; Li *et al.* 2023). Additionally, the β-hydroxybutyrate challenge was successful in simulating the ketotic phenotype, *id est*, MAC-T cells accumulated TAG and had higher abundance of SREBP1, ACACA, FASN, SCD1, DGAT1, PPARγ and DGAT2 along with lower abundance of the fatty acid oxidation-related proteins PPARα, PGC-1α and CPT1A. Our discovery that BHB challenge also led to increased ACSL4 levels in BMECs underscored that this protein has a biological function in the control of fatty acid content and lipid droplet accumulation. The fact that inhibition of ACSL4 significantly lowered the abundance of fatty acid synthesis-related proteins while increasing fatty acid oxidation-related proteins confirmed data from nonruminant models. In contrast, overexpression ACSL4 could increase the abundance of fatty acid synthesis-related proteins and lipid droplet accumulation with or without BHB treatment. These results suggested that ACSL4 could enhance BHB-induced fatty acid synthesis signaling pathway in MAC-T cells. Thus, *in vivo* and *in vitro* experiments allowed us to accomplish our main goals with respect to ACSL4, a protein that is crucial for increased fatty acid content and lipid droplet accumulation (Fan *et al.* 2020; Ren *et al.* 2022).

Although fatty acid content is increased in ketotic dairy cows that have high blood concentrations of BHB (Duffield *et al.* 2009; Zhang *et al.* 2020), this condition reduces milk yield, which underscores that excessive BHB may cause negative effects within the mammary gland. Mechanistically, the greater abundance of FA synthesis-related proteins ACSL4, SREBP1, ACACA, FASN, SCD1, DGAT1 and DGAT2 in ketotic dairy cows and MAC-T cells challenged with high levels of BHB was consistent with earlier results (Duffield *et al.* 2009; Zhang *et al.* 2020). Research on non-ruminants has demonstrated that ACSL4 directly influences lipid droplet accumulation by altering fatty acid metabolism (Chen *et al.* 2021; Ren *et al.* 2022). Thus, the fact that ACSL4 silencing in mammary cells *via* siRNA markedly decreased mRNA and protein abundance of SREBP1, ACACA, FASN, SCD1, DGAT1 and DGAT2 while reducing lipid droplet accumulation induced by BHB suggest a role for ACSL4 in increasing fatty acid content and lipid droplet accumulation in BMECs.

Fatty acid oxidation is an important biological mechanism that helps regulate energy availability to the mammary gland. During the β-oxidation process, fatty acid entry into mitochondria is controlled by CPT1A activity (Li *et al.* 2013). Further, at least in nonruminants, PPARα regulates mitochondrial β-oxidation and fatty acid transport (Pawlak *et al.* 2015). Previous studies have shown that fatty acid β-oxidation capability in dairy cows with ketosis is significantly reduced (Li *et al.* 2012). Thus, the decrease in protein abundance of PPARα and PGC-1α in response to BHB revealed an imbalance between FA synthesis and FA oxidation. In addition, inhibition of ACSL4 mitigated the downregulation in abundance of CPT1A, PPARα and PGC-1α induced by BHB, suggesting that it plays a regulatory role in FA oxidation. Thus, ACSL4 increased fatty acid content is a major pathway that competes with CPT1A, PPARα and PGC-1α for utilization of fatty acids for oxidation.

Dairy cows with severe NEB experience mitochondrial dysfunction in mammary cells, which in turn lowers secretory capacity. Increased fatty acid oxidation could prevent lipid droplet accumulation and, hence, lower lipotoxicity (Duan *et al.* 2022). Thus, promoting mitochondrial function and enhancing fatty acid oxidation should be the most effective strategies to protect mammary epithelial cells from lipotoxicity. The transcription coactivator PGC-1α is responsible for the regulation of mitochondrial function in nonruminants (Kelly and Scarpulla 2004). The lower mRNA and protein abundance of PGC-1α after BHB treatment along with reduced MMP level underscored the reduction in mitochondrial function. Furthermore, inhibition of ACSL4 during BHB challenge alleviated mitochondrial functional impairment and upregulated PGC-1α abundance. Thus, combined with the increase in ACSL4 after BHB treatment and the previous reports that ACSL4 knockdown promotes PGC1α expression in mice (Yadav *et al.* 2011), these data suggested that ACSL4 may regulate FA oxidation through PGC-1α in BMECs. These result prompts us to speculate that lowering ACSL4 could play a dominant role in reducing fatty acid content and regulating FA oxidation to protect cells from lipotoxicity.

5. Conclusion

In bovine mammary epithelial cells, ACSL4 appears to play an essential role in increasing fatty acid content and lipid droplet accumulation while diminishing the ability for FA β-oxidation and proper mitochondrial function. As a result, alterations in abundance of ACSL4 could serve to regulate the abnormal fatty acid metabolism during periods where concentrations of circulating BHB increase markedly.

Acknowledgements

The study was supported by the grants from the National Key Research and Development Program of China (2023YFD1800804 and 2023YFD1801100), the National Natural Science Foundation of China (32172926), and the China Agriculture Research System (CARS-36).

Declaration of competing interest

The authors declare that they have no conflict of interest.

Declaration of generative AI and AI-assisted technologies in the writing process

The authors declare that they did not use AI in the preparation and writing of this manuscript.

Ethical approval

The animal use and care procedures were approved by the Heilongjiang Bayi Agricultural University Ethics Committee for the Use and Care of Animals (Daqing, China, approval number: SY202206021).

Data availability

The datasets used and/or analyzed during the current study are publicly available.

Appendix associated with this study is available at https://doi.org/10.1016/j.jia.2024.12.004

References

Baird G D. 1982. Primary ketosis in the high-producing dairy cow: Clinical and subclinical disorders, treatment, prevention, and outlook. *Journal of Dairy Science*, **65**, 1–10.

Bauman D E, Griinari J M. 2000. Regulation and nutritional manipulation of milk fat. Low-fat milk syndrome. *Advances in Experimental Medicine and Biology*, **480**, 209–216.

Bionaz M, Loor J J. 2008a. ACSL1, AGPAT6, FABP3, LPIN1, and SLC27A6 are the most abundant isoforms in bovine mammary tissue and their expression is affected by stage of lactation. *Journal of Nutrition*, **138**, 1019–1024.

Bionaz M, Loor J J. 2008b. Gene networks driving bovine milk fat synthesis during the lactation cycle. *BMC Genomics*, **9**, 366.

Chen J, Ding C, Chen Y, Hu W, Yu C, Peng C, Feng X, Cheng Q, Wu W, Lu Y, Xie H, Zhou L, Wu J, Zheng S. 2021. ACSL4 reprograms fatty acid metabolism in hepatocellular carcinoma *via* c-Myc/SREBP1 pathway. *Cancer Letters*, **502**, 154–165.

Duan J, Wang Z, Duan R, Yang C, Zhao R, Feng Q, Qin Y, Jiang J, Gu S, Lv K, Zhang L, He B, Birnbaumer L, Yang S, Chen Z, Yang Y. 2022. Therapeutic targeting of hepatic ACSL4 ameliorates NASH in mice. *Hepatology*, **75**, 140–153.

Duffield T F, Lissemore K D, McBride B W, Leslie K E. 2009. Impact of hyperketonemia in early lactation dairy cows on health and production. *Journal of Dairy Science*, **92**, 571–580.

Fan Y, Han Z, Lu X, Zhang H, Arbab A A I, Loor J J, Yang Y, Yang Z. 2020. Identification of milk fat metabolism-related pathways of the bovine mammary gland during mid and late lactation and functional verification of the ACSL4 gene. *Genes* (Basel), **11**, 1357.

Finck B N, Gropler M C, Chen Z, Leone T C, Croce M A, Harris T E, Lawrence Jr J C, Kelly D P. 2006. Lipin 1 is an inducible amplifier of the hepatic PGC–1alpha/PPARalpha regulatory pathway. *Cell Metabolism*, **4**, 199–210.

Jia J, Duan H, Liu B, Ma Y, Ma Y, Cai X. 2023. Alfalfa Xeno-miR168b Target CPT1A to regulate milk fat synthesis in bovine mammary epithelial cells. *Metabolites*, **13**, 76.

Kadegowda A K, Bionaz M, Piperova L S, Erdman R A, Loor J J. 2009. Peroxisome proliferator-activated receptor-gamma activation and long-chain fatty acids alter lipogenic gene networks in bovine mammary epithelial cells to various extents. *Journal of Dairy Science*, **92**, 4276–4289.

Kelly D P, Scarpulla R C. 2004. Transcriptional regulatory circuits controlling mitochondrial biogenesis and function. *Genes and Development*, **18**, 357–368.

Kotronen A, Yki-Jarvinen H, Aminoff A, Bergholm R, Pietilainen K H, Westerbacka J, Talmud P J, Humphries S E, Hamsten A, Isomaa B, Groop L, Orho-Melander M, Ehrenborg E, Fisher R M. 2009. Genetic variation in the *ADIPOR2* gene is associated with liver fat content and its surrogate markers in three independent cohorts. *European Journal of Endocrinology*, **160**, 593–602.

Li J, Zhao C, Liu M, Chen L, Zhu Y, Gao W, Du X, Song Y, Li X, Liu G, Lei L, Feng H. 2023. Nuciferine ameliorates nonesterified fatty Acid-Induced bovine mammary epithelial cell lipid accumulation, apoptosis, and impaired migration *via* activating LKB1/AMPK signaling pathway. *Journal of Agricultural and Food Chemistry*, **71**, 443–456.

Li P, Li X B, Fu S X, Wu C C, Wang X X, Yu G J, Long M, Wang Z, Liu G W. 2012. Alterations of fatty acid beta-oxidation capability in the liver of ketotic cows. *Journal of Dairy Science*, **95**, 1759–1766.

Li P, Wu C C, Long M, Zhang Y, Li X B, He J B, Wang Z, Liu G W. 2013. Short communication: High insulin concentrations inhibit fatty acid oxidation-related gene expression in calf hepatocytes cultured *in vitro*. *Journal of Dairy Science*, **96**, 3840–3844.

Littledike E T, Young J W, Beitz D C. 1981. Common metabolic diseases of cattle: Ketosis, milk fever, grass tetany, and downer cow complex. *Journal of Dairy Science*, **64**, 1465–1482.

Liu X, Shen J, Zong J, Liu J, Jin Y. 2021. Beta-Sitosterol promotes milk protein and fat syntheses-related genes in bovine mammary epithelial cells. *Animals* (Basel), **11**, 3238.

Loor J J, Bionaz M, Drackley J K. 2013. Systems physiology in dairy cattle: Nutritional genomics and beyond. *Annual Review of Animal Biosciences*, **1**, 365–392.

NASEM (National Academies of Sciences, Engineering, and Medicine of the United States). 2021. In: *Nutrient Requirements of Dairy Cattle*: *Eighth Revised Edition*. National Academies of Sciences, Engineering, and Medicine, Washington, D.C.

Oetzel G R. 2004. Monitoring and testing dairy herds for metabolic disease. *Veterinary Clinics of North America-Food Animal Practice*, **20**, 651–674.

Pawlak M, Lefebvre P, Staels B. 2015. Molecular mechanism of PPARalpha action and its impact on lipid metabolism, inflammation and fibrosis in non-alcoholic fatty liver disease. *Journal of Hepatology*, **62**, 720–733.

Ren H, Zhang H, Hua Z, Zhu Z, Tao J, Xiao H, Zhang L, Bi Y, Wang H. 2022. ACSL4 directs intramuscular adipogenesis and fatty acid composition in pigs. *Animals* (Basel), **12**, 119.

Steenson S, Shojaee-Moradie F, Whyte M B, Jackson K G, Lovegrove J A, B A F, Umpleby A M. 2020. The effect of fructose feeding on intestinal triacylglycerol production and *de novo* fatty acid synthesis in Humans. *Nutrients*, **12**, 1781.

Sun X, Wang Y, Loor J J, Bucktrout R, Shu X, Jia H, Dong J, Zuo R, Liu G, Li X, Li X. 2019. High expression of cell death-inducing DFFA-like effector a (CIDEA) promotes milk fat content in dairy cows with clinical ketosis. *Journal of Dairy Science*, **102**, 1682–1692.

Tuohetahuntila M, Spee B, Kruitwagen H S, Wubbolts R, Brouwers J F, van de Lest C H, Molenaar M R, Houweling M, Helms J B, Vaandrager A B. 2015. Role of long-chain acyl-CoA synthetase 4 in formation of polyunsaturated lipid species in hepatic stellate cells. *Biochimica et Biophysica Acta*, **1851**, 220–230.

Yadav H, Quijano C, Kamaraju A K, Gavrilova O, Malek R, Chen W, Zerfas P, Zhigang D, Wright E C, Stuelten C, Sun P, Lonning S, Skarulis M, Sumner A E, Finkel T, Rane S G. 2011. Protection from obesity and diabetes by blockade of TGF-beta/Smad3 signaling. *Cell Metabolism*, **14**, 67–79.

Zhang B, Li M, Yang W, Loor J J, Wang S, Zhao Y, Guo H, Ma X, Xia C, Xu C. 2020. Orai calcium release-activated calcium modulator 1 (ORAI1) plays a role in endoplasmic reticulum stress in bovine mammary epithelial cells challenged with physiological levels of ketone bodies. *Journal of Dairy Science*, **103**, 4691–4701.

Zhang S, Qi H, Wen X P, Li P, Gao X J, Ao J X. 2019. The phosphorylation of Tudor-SN mediated by JNK is involved in the regulation of milk protein synthesis induced by prolactin in BMECs. *Journal of Cellular Physiology*, **234**, 6077–6090.

Zhu J, Cui G, Chen M, Xu Q, Wang X, Zhou D, Lv S, Fu L, Wang Z, Zuo J. 2013. Expression of R132H mutational IDH1 in human U87 glioblastoma cells affects the SREBP1a pathway and induces cellular proliferation. *Journal of Molecular Neuroscience*, **50**, 165–171.

Zhu Y, Guan Y, Loor J J, Sha X, Coleman D N, Zhang C, Du X, Shi Z, Li X, Wang Z, Liu G, Li X. 2019. Fatty acid-induced endoplasmic reticulum stress promoted lipid accumulation in calf hepatocytes, and endoplasmic reticulum stress existed in the liver of severe fatty liver cows. *Journal of Dairy Science*, **102**, 7359–7370.

Executive Editor-in-Chief Dongming Zhao
Managing Editor Han Zhang